ELSEVIER

Carbohydrate Research 279 (1995) 21–39

CARBOHYDRATE RESEARCH

Synthesis and conformational analysis of the Amadori compound *N*-(2,3:4,5-di-*O*-isopropylidene-1-deoxy-β-D-fructopyranos-1-yl)-L-tyrosine benzyl ester

Biserka Kojić-Prodić [a,*], Vjekoslav Milinković [a], Jurka Kidrič [b], Primož Pristovšek [b], Štefica Horvat [a], Andreja Jakas [a]

[a] *Rudjer Bošković Institute, P.O.B. 1016, 41001 Zagreb, Croatia*
[b] *National Institute of Chemistry, P.O.B. 30, 61015 Ljubljana, Slovenia*

Received 4 April 1995; accepted 14 July 1995

Abstract

The title compound, a precursor in the synthesis of other analogues of Amadori type, was prepared and characterized by X-ray structure analysis and NMR spectroscopy. The molecule crystallized in the orthorhombic space group $P2_12_12_1$ with $a = 10.441(2)$, $b = 10.894(2)$, $c = 24.686(4)$Å, $Z = 4$. The molecule is flexible even in solid state; at 100 K two orientations of the benzyloxy group are present in the unit cell. Therefore, molecular mechanics and molecular dynamics simulations were used to study its conformational changes. The results obtained were compared with experimental observations. The comparative analysis revealed that the two conformers detected in the crystal are different from the energetically favourable conformations in Me_2SO solutions. Rotations about both C–N bonds affect the global molecular conformation. The β-D-fructopyranose moiety blocked with two dioxolane rings is the less flexible part of the molecule; in the solid state and in Me_2SO-d_6 it is in the *skew* conformation.

Keywords: Amadori compound; Maillard products; Synthesis; *N*-(2,3:4,5-Di-*O*-isopropylidene-1-deoxy-β-D-fructopyranos-1-yl)-L-tyrosine benzyl ester; X-ray structure; NMR spectroscopy; Molecular dynamics

* Corresponding author.

SSDI 0008-6215(95)00255-3

1. Introduction

The interaction between glucose, as well as other reducing sugars, and amino acids or proteins (Maillard reaction) is a topic of a wide interest, ranging from food chemistry to medicine [1]. The early step in this reaction assumes that the Schiff base resulting from the initial sugar attachment to the primary amino group undergoes an Amadori rearrangement to yield *N*-(1-deoxy-D-fructos-1-yl) product. This Amadori compound is degraded into a series of reactive compounds that act as propagators of denaturation, polymerization and cross-linking of tissue proteins in vivo [2]. For human health, this reaction is of interest for two main reasons. First, the Maillard reaction occurs extensively during food preparation where it affects nutritional quality and may be accompanied by the formation of toxic substances [1,3] and second, the Maillard reaction has been suggested to be involved in the tissue ageing process [4,5] and diabetic complications [6]. The exact role of the Maillard reaction in the overall ageing process remains a matter of speculation, but the inter-relationship between the time-related appearance of Maillard reaction-related cross-links in proteins, cells and tissues and the overall ageing process appears indisputable [7]. A recently published paper on preparation and characterization of 1-amino-1-deoxy-D-fructose derivatives derived from a series of aliphatic ω-amino acids [8] is indicative of a wide interest for this class of compounds.

In order to obtain information on the conformational behaviour of the *N*-(1-deoxy-D-fructos-1-yl) derivative of L-tyrosine we prepared and structurally characterized the fully protected Amadori compound **1** which is described here.

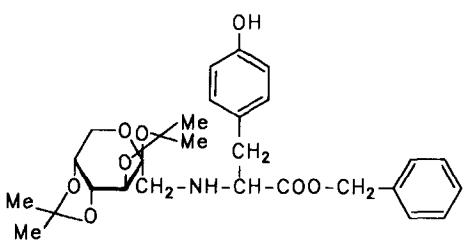

1

The X-ray structure analysis was used to uniquely define molecular configuration and conformation in the solid state. The results obtained were compared with NMR spectroscopy parameters of the compound and were used together with molecular dynamics (MD) simulations for comparative conformational analysis.

2. Results and discussion

The conformational characteristics have been examined in different media: in the crystal by X-ray analysis and in Me_2SO-d_6 by NMR spectroscopy as well as molecular dynamics simulations (MD) in vacuo and in Me_2SO. The molecule exhibits an am-

phipatic character with more pronounced hydrophobic characteristics and it is not soluble in water.

X-Ray structure analysis.—The structure with atom numbering is shown in Fig. 1. The ORTEP [9] plot is drawn with thermal ellipsoids at the 30% level. Selected bond lengths and angles are listed in Table 1. Data collected at 100 K revealed two equally populated orientations of the benzyloxy group whereas in the room-temperature data more orientations were recognized; the molecule with two orientations of the benzyloxy group in the crystal is shown in Fig. 2. The conformation of the molecule is described by selected torsion angles (Table 2) and asymmetry parameters [10] listed for the β-D-fructopyranose and dioxolane rings (Table 3). Conformational changes caused the phase transition which was detected at 114 K. It was accompanied by a small change of the heat capacity ($C_p = 0.025$ J/g/K). The room-temperature polymorph has a more disordered structure than the low-temperature one; thus the low-temperature data have been presented only.

The molecular geometry of the sugar moiety is in agreement with the results published for 2,3:4,5-di-*O*-isopropylidene-β-D-fructopyranose (with two independent molecules in asymmetric units) [11], therefore it will be briefly summarized only. The endo-cyclic bonds in the β-D-fructopyranose ring [O-6–C-6, 1.437(4); O-6–C-2, 1.387(5) Å] are asymmetric; the endo-cyclic angle C-2–O-6–C-6 is 113.4(2)°. The conformational analysis of β-D-fructopyranose and dioxolane rings is based on asymmetry parameters [10] (Table 3). In accordance with the convention of IUPAC-IUB (JCBN) [12] and the original paper of Schwarz [13] the conformation of the β-D-fructopyranose ring in the crystal is described as *skew* (Table 3). The protection of β-D-fructopyranose with isopropylidene groups caused a distortion of the ring. The analysis upon Boeyens

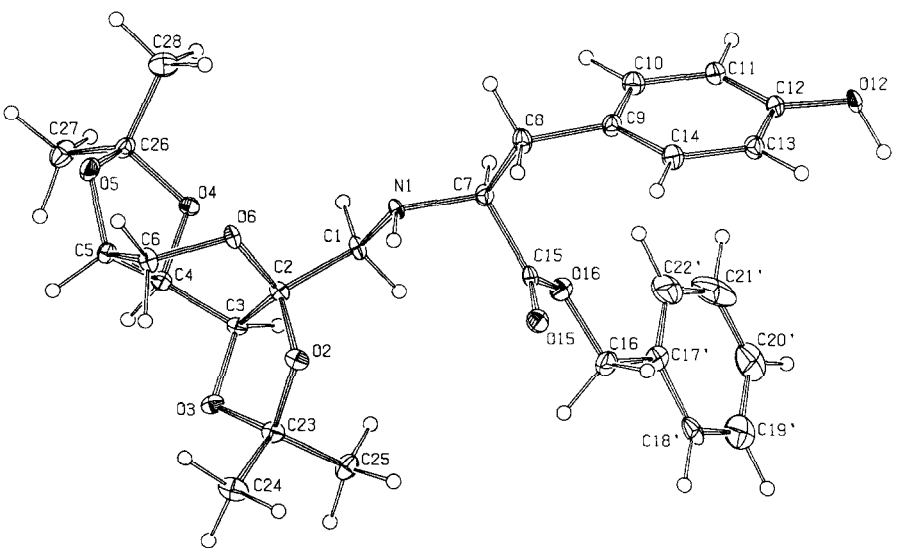

Fig. 1. Molecular structure (ORTEP drawing) with one of two detected conformers and atom numbering. The thermal ellipsoids are drawn at a 30% probability level.

Table 1
Selected bond lengths (Å) and angles (°)

Sugar residue			
C-2–C-3	1.552(4)	C-2–O-6–C-6	113.4(2)
C-3–C-4	1.518(5)	C-2–C-3–C-4	113.5(3)
C-4–C-5	1.546(4)	C-3–C-4–C-5	114.1(3)
C-5–C-6	1.508(5)	C-4–C-5–C-6	112.7(3)
O-6–C-6	1.437(4)	O-6–C-6–C-5	110.5(2)
O-6–C-2	1.387(5)	C-2–O-2–C-23	110.1(3)
O-2–C-2	1.435(4)	C-3–O-3–C-23	106.6(3)
O-2–C-23	1.449(5)	O-2–C-23–C-24	109.5(3)
O-3–C-3	1.429(4)	O-2–C-23–C-25	109.1(4)
O-3–C-23	1.432(5)	O-2–C-23–O-3	103.8(3)
C-23–C-24	1.498(7)	O-3–C-23–C-24	108.7(4)
C-23–C-25	1.530(6)	O-3–C-23–C-25	111.4(3)
O-4–C-4	1.428(4)	C-24–C-23–C-25	113.9(4)
O-4–C-26	1.433(4)	C-4–O-4–C-26	106.1(3)
O-5–C-5	1.423(4)	C-5–O-5–C-26	109.0(2)
O-5–C-26	1.423(5)	O-4–C-26–C-27	110.5(3)
C-26–C-27	1.508(6)	O-4–C-26–C-28	107.4(4)
C-26–C-28	1.505(7)	O-4–C-26–O-5	105.3(3)
		O-5–C-26–C-27	110.4(4)
		O-5–C-26–C-28	109.0(3)
		C-27–C-26–C-28	113.9(4)
		O-2–C-2–O-6	109.4(2)
		O-2–C-2–C-1	111.2(3)
		O-2–C-2–C-3	103.2(3)
		O-6–C-2–C-1	107.3(3)
		O-6–C-2–C-3	114.9(3)
		C-1–C-2–C-3	110.9(3)
		O-3–C-3–C-2	104.1(2)
		O-3–C-3–C-4	108.3(2)
		O-4–C-4–C-3	106.7(2)
		O-4–C-4–C-5	103.1(2)
		O-5–C-5–C-4	104.7(2)
		O-5–C-5–C-6	109.4(3)
Aliphatic chain			
C-1–C-2	1.523(4)	C-2–C-1–N-1	112.1(3)
N-1–C-1	1.466(5)	C-1–N-1–C-7	111.2(3)
N-1–C-7	1.475(4)	N-1–C-7–C-8	111.2(3)
C-7–C-8	1.542(5)	N-1–C-7–C-15	110.2(2)
C-8–C-9	1.527(3)	C-7–C-8–C-9	110.5(3)
C-7–C-15	1.538(5)	C-8–C-7–C-15	108.9(3)
O-15–C-15	1.189(5)	C-8–C-9–C-10	119.3(2)
O-16–C-15	1.348(5)	C-8–C-9–C-14	120.5(2)
O-16–C-16	1.453(5)	O-12–C-12–C-11	118.4(1)
C-16–C-17	1.431(9)	O-12–C-12–C-13	121.4(1)
C-16–C-17′	1.574(8)	C-15–O-16–C-16	114.2(3)
		O-15–C-15–O-16	124.5(3)
		O-15–C-15–C-7	124.4(4)
		O-16–C-15–C-7	111.1(3)
		O-16–C-16–C-17	107.2(5)
		O-16–C-16–C-17′	107.5(4)

Table 1 (continued)

		C-16–C-17–C-18	124.0(5)
		C-16–C-17–C-22	115.9(6)
		C-16–C-17′–C-18′	115.8(5)
		C-16–C-17′–C-22′	124.2(5)
Tyrosine moiety			
C-9–C-10	1.3951(1)		
C-9–C-14	1.3949(1)		
C-10–C-11	1.3950(1)		
C-11–C-12	1.3949(1)		
O-12–C-12	1.364(3)		
C-12–C-13	1.3948(1)		
C-13–C-14	1.3946(1)		
Ester group			
C-17–C-18	1.396(9)		
C-18–C-19	1.395(10)		
C-19–C-20	1.396(7)		
C-20–C-21	1.394(9)		
C-17–C-22	1.394(7)		
C-21–C-22	1.395(10)		
C-17′–C-18′	1.395(9)		
C-18′–C-19′	1.394(8)		
C-19′–C-20′	1.396(8)		
C-20′–C-21′	1.394(9)		
C-17′–C-22′	1.395(8)		
C-21′–C-22′	1.395(8)		

The tyrosine moiety was treated as a rigid group.

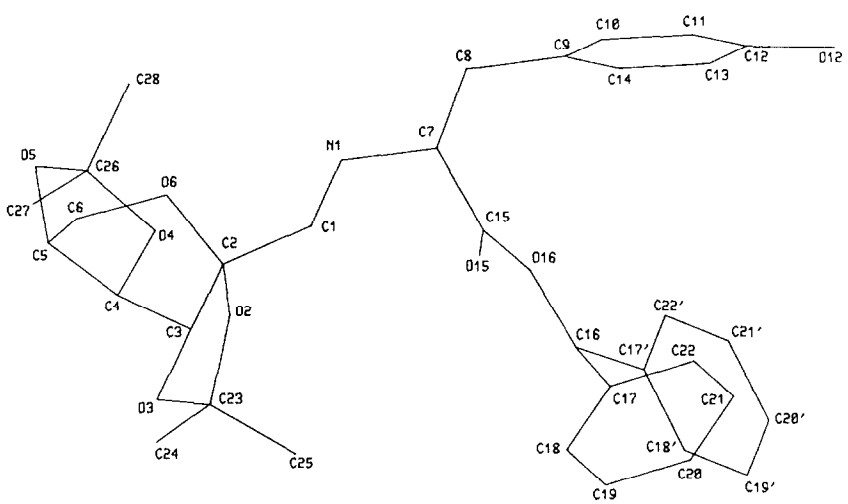

Fig. 2. Skeleton of the molecule with two orientations of benzyloxy group detected in the crystalline state.

criteria [14] and Cremer and Pople [15] parameters detected an intermediate *screw–boat / twist–boat* conformation having C-3 [0.28(2) Å], C-6 [0.37(2) Å] and O-6 [0.36(2) Å] displaced from the best least-squares plane through the six atoms of the ring. This intermediate conformation (Table 3) was also detected in 2,3:4,5-di-*O*-isopropylidene-β-D-fructopyranose [11] and 31 structures (quotations included in the ref. [16]) of 1,2:3,4-di-*O*-isopropylidene galactopyranose and related systems [16] extracted from the Cam-

Table 2
Selected torsion angles (°)

Sugar residue	
C-2–C-3–C-4–C-5	−41.7(3)
C-2–O-6–C-6–C-5	−69.4(4)
C-3–C-4–C-5–C-6	13.6(3)
C-4–C-5–C-6–O-6	39.3(4)
C-6–O-6–C-2–C-3	39.0(3)
O-6–C-2–C-3–C-4	16.2(3)
C-2–C-3–C-4–O-4	71.5(3)
C-2–O-2–C-23–C-24	−139.4(3)
C-2–O-2–C-23–C-25	95.4(3)
C-2–O-2–C-23–O-3	−23.5(4)
C-3–O-3–C-23–C-24	151.6(3)
C-3–O-3–C-23–C-25	−82.1(4)
C-3–O-3–C-23–O-2	35.2(4)
C-3–C-4–C-5–O-5	132.5(2)
O-2–C-2–C-3–C-4	135.2(2)
O-2–C-2–C-3–O-3	17.6(3)
C-23–O-2–C-2–C-3	3.6(3)
C-23–O-2–C-2–O-6	126.4(3)
C-23–O-2–C-2–C-1	−115.3(3)
C-23–O-3–C-3–C-2	−32.9(3)
C-23–O-3–C-3–C-4	−154.0(3)
C-4–O-4–C-26–O-5	34.8(4)
C-4–O-4–C-26–C-27	−84.4(4)
C-4–O-4–C-26–C-28	150.9(3)
C-5–O-5–C-26–C-28	−138.2(3)
C-5–O-5–C-26–O-4	−23.3(4)
C-5–O-5–C-26–C-27	96.0(3)
C-26–O-4–C-4–C-5	−31.6(3)
C-26–O-5–C-5–C-6	124.7(3)
C-26–O-5–C-5–C-4	3.6(3)
C-26–O-4–C-4–C-3	−152.1(3)
O-6–C-2–C-3–O-3	−101.4(3)
O-3–C-3–C-4–C-5	73.4(3)
O-3–C-3–C-4–O-4	−173.4(2)
O-4–C-4–C-5–C-6	−101.7(3)
O-4–C-4–C-5–O-5	17.2(3)
O-5–C-5–C-6–O-6	−76.8(3)
C-6–O-6–C-2–O-2	−76.4(3)
C-6–O-6–C-2–C-1	162.9(3)
C-1–C-2–C-3–C-4	−105.7(3)
C-1–C-2–C-3–O-3	136.7(3)

Table 2 (continued)

Aliphatic chain	
C-1–N-1–C-7–C-8	170.8(3)
C-1–N-1–C-7–C-15	−68.3(4)
C-7–N-1–C-1–C-2	158.3(3)
C-7–C-8–C-9–C-10	61.8(3)
C-7–C-8–C-9–C-14	−113.3(2)
C-8–C-7–C-15–O-15	57.8(4)
C-8–C-7–C-15–O-16	−122.5(3)
C-8–C-9–C-10–C-11	−175.1(2)
C-8–C-9–C-14–C-13	175.1(2)
N-1–C-1–C-2–C-3	176.9(3)
N-1–C-1–C-2–O-2	−68.9(4)
N-1–C-1–C-2–O-6	50.6(4)
N-1–C-7–C-8–C-9	−178.4(2)
C-15–C-7–C-8–C-9	59.9(3)
N-1–C-7–C-15–O-16	115.2(3)
N-1–C-7–C-15–O-15	−64.5(5)
C-16–O-16–C-15–O-15	−0.7(5)
C-16–O-16–C-15–C-7	179.7(3)
C-10–C-11–C-12–O-12	175.0(2)
O-12–C-12–C-13–C-14	−174.9(2)
O-16–C-16–C-17–C-18	−91.1(9)
O-16–C-16–C-17–C-22	90.1(8)
C-16–C-17–C-18–C-19	−178.8(8)
C-16–C-17–C-22–C-21	178.8(8)
C-15–O-16–C-16–C-17	172.0(4)
O-16–C-16–C-17′–C-18′	−169.6(5)
O-16–C-16–C-17′–C-22′	11.5(7)
C-16–C-17′–C-18′–C-19′	−179.0(5)
C-16–C-17′–C-22′–C-21′	178.9(5)
C-15–O-16–C-16–C-17′	−165.5(3)

bridge Structural Database [17]. The expanded convention of carbohydrate nomenclature has been proposed [16] and this very conformation accordingly described as an intermediate *screw–boat / twist–boat*. The dioxolane rings retain an *envelope* conformation; the bond lengths C–O in the dioxolane rings (Table 1) correspond to the value of a single bond (1.428 Å) [18]. However, the valence angles at the atoms O-3 and O-4 of dioxolane rings in their puckered parts (*envelope*, Table 3) considerably deviate from the value required by hybridization [C-3–O-3–C-23, 106.6(3)°; C-4–O-4–C-26, 106.1(3)°]. This deformation is imposed by requirements of the five-membered ring geometry.

The overall molecular conformation is defined by the relative orientations of the sugar and the tyrosine moieties and the ester group. Along the aliphatic zig-zag backbone the conformation about C-1–N-1, N-1–C-7 and C-7–C-8 is (±) antiperiplanar (Table 2) [19]. The orientation of the ester group towards the glyco-amino acid part is defined by the torsion angle with the atom sequence N-1–C-7–C-15–O-16, 115.2(3)°. The benzyloxy group is embedded into the space available in the crystal lattice in two

Table 3
Ring conformation analysis based on asymmetry parameters [10] values using X-ray data of the title compound and its sugar analogue [11]

Atom sequence	Asymmetry parameters [10]	Cremer–Pople parameters [15]	Conformation
Dioxolane rings			
O-2–C-2–C-3–O-3–C-23	ΔC_s (O-3) = 4.5°	Q = 0.322(3) Å ϕ = 112.36(6)°	*envelope*
O-4–C-4–C-5–O-5–C-26	ΔC_s (O-4) = 4.9°	Q = 0.314(3) Å ϕ = 355.5(6)°	*envelope*
β-D-fructopyranose ring			
C-2–C-3–C-4–C-5–C-6–O-6	ΔC_2(C-3–C-4) = 1.9°	Q = 0.643(3) Å ϕ = 147.3(3)° Θ = 98.5(3)°	*skew*
Molecule A [a]			
Dioxolane rings			
O-2–C-2–C-3–O-3–C-23	ΔC_s (O-3) = 4.3°	Q = 0.326(5) Å ϕ = 78.9(7)°	*envelope*
O-4–C-4–C-5–O-5–C-26	ΔC_2(O-5) = 4.0° ΔC_s(O3) = 6.9°	Q = 0.239(5) Å ϕ = 166(1)°	*twist / envelope*
β-D-fructopyranose ring			
C-2–C-3–C-4–C-5–C-6–O-6	ΔC_2(C-3–C-4) = 2.2°	Q = 0.664(5) Å ϕ = 147.5(4)° Θ = 97.0(4)°	*skew*
Molecule B [a]			
Dioxolane rings			
O-2–C-2–C-3–O-3–C-23	ΔC_s (O-3) = 3.4°	Q = 0.323(5) Å ϕ = 77.9(7)°	*envelope*
O-4–C-4–C-5–O-5–C-26	ΔC_s (O-3) = 3.4°	Q = 0.278(5) Å ϕ = 173(1)°	*envelope*
β-D-fructopyranose ring			
C-2–C-3–C-4–C-5–C-6–O-6	ΔC_2(C-3–C-4) = 1.5°	Q = 0.653(5) Å ϕ = 149.1(5)° Θ = 96.5(5)°	*skew*

[a] Two molecules in asymmetric unit [11].

orientations (with equal populations). The phenyl ring is either perpendicular to or parallel with the plane C-15–O-16–C-16 (Fig. 2). The two orientations detected even at 100 K suggest a pronounced flexibility of this group that is reflected on the parameters of the thermal ellipsoids (Fig. 1).

Crystal packing and hydrogen bonds.—The conformational changes in the ester portion of the molecule introduce a disorder which might be of statistical or dynamical character. High thermal motion of the ester group (Fig. 1) present at 100 K might suggest dynamical disorder. The overcrowded effect recognized in one of two detected orientations of the benzyloxy group can be the reason for disorder detected at room-temperature and at 100 K. Crystal packing is dominated by the very complex system of the three-dimensional hydrogen bond network (Table 4). The amino group acts both as a

Table 4
Hydrogen bond geometry

	$D \cdots A$ (Å)	D–H (Å)	H $\cdots A$ (Å)	D–H $\cdots A$ (°)	Symmetry operation on A
N-1–H-1 $\cdots$ O-3	3.054(4)	1.00(3)	2.09(2)	161(2)	$1/2+x, 1/2-y+1, -z$
O-12–H $\cdots$ N-1	2.770(5)	0.98(3)	1.83(3)	159(2)	$-x+1, 1/2+y, 1/2-z$

donor to the oxygen atom of the dioxolane ring (O-3) and as an acceptor for the tyrosine OH group. The hydrogen bond N-1–H $\cdots$ O-3 forms the spirals along *a* whereas O-12–H $\cdots$ N-1 connects them in direction *b*. The aggregation of these two motifs forms a chain in the [111] direction.

NMR spectroscopy in Me_2SO-d_6.—The assignments of ^1H and ^{13}C resonances. The assignment of ^1H and ^{13}C chemical shifts was accomplished using the 1D and 2D experiments mentioned in the Experimental section; comparison with the spectra of analogues [20–22] was also used. Chemical shifts, coupling constants and NOE connectivities are given in Tables 5–7.

From the COSY spectrum it was easy to assign H-31 which has only one correlation, namely with H-41 which correlates with H-51, and this one with H-61, H-62. C-8–H-81, H-82 was distinguished from C-16–H-16′, H-16″ and N-1–C-1–H-11, H-12 on the basis of its correlation with N-1–C-7–H-71. The multiplet of H-71 is of the ABMX type and unfortunately overlaps with H-61, so only the estimates of $J_{71,81}$ and $J_{71,82}$ can be deduced by decoupling of H-1 (Table 6). The four methyl groups of the *O*-isopropylidene rings have different chemical shifts. Three of them have an NOE connectivity with a particular proton of the sugar ring (Table 7). The protons H-41 and H-51 have the NOE connectivity with the methyl-protons at 1.27 ppm, the proton H-3 with the methyl-protons at 1.30 ppm and the methylene proton on C-6 at 3.71 ppm with the methyl-protons at 1.41 ppm. The COLOC experiment gives the correlations between the quaternary carbons at 107.4 and 107.9 ppm and the methyl-protons at 1.27, 1.41 and 1.30 ppm, respectively.

Taking into the account the distances of the sugar ring protons to the geometrical centres of isopropylidene methyl groups (Table 8) the resonance signals at 1.27 ppm and 1.30 ppm can be assigned to C-27H_3 and C-25H_3 methyl groups, respectively. The other two isopropylidene methyl groups C-24H_3 and C-28H_3 can be assigned from the COLOC spectrum via their correlation with the quaternary carbons C-23 and C-26. C-2 was assigned via the long range couplings with H-11, H-12 and H-41.

^1H chemical shifts of compound **1** in Me_2SO-d_6 are close to those reported by Lopez and Gruenwedel for aromatic Amadori compounds in $CDCl_3$ [20]. The C-1 resonance signal in **1** is found at 51.8 ppm, the characteristic value of other nonprotected Amadori compounds with a secondary N-atom [22]. The resonance signals of C-2 to C-6 are comparable to those reported for disaccharides with a 2,3;4,5-di-*O*-isopropylidene-D-fructopyranose group [23].

Conformational analysis. ^1H spectra of **1** show several characteristic features that may be associated with the conformations adopted by **1** in Me_2SO-d_6.

Table 5
Chemical shifts δ_H and $\delta_{^{13}C}$ (ppm) of **1** in Me_2SO-d_6

Atoms	δ_H	$\delta_{^{13}C}$
N-1–H-1	2.08	
C-1–H-11, H-12	2.67	51.8
C-2		103.2
C-3–H-31	4.29	70.2
C-4–H-41	4.53	69.6
C-5–H-51	4.19	70.3
C-6–H-61, H-62	3.52, 3.71	60.4
C-7–H-71	3.56	63.3
C-8–H-81, H-82	2.76	37.7
C-9		135.9
C-10–H-101	6.91	130.0
C-11–H-111	6.64	115.0
C-12–O-12–H-2	9.22	155.9
C-13–H-131	6.64	115.0
C-14–H-141	6.91	130.0
C-15		173.6
C-16–H-16′, H-16″	5.02	65.4
C-17′		128.3
C-18′–H-18′	7.20	128.3
C-19′–H-19′	7.34	128.0
C-20′–H-20′	7.34	128.0
C-21′–H-21′	7.34	128.0
C-22′–H-22′	7.20	128.3
C-23		107.9
C-24–H_3	1.33	25.7
C-25–H_3	1.30	25.4
C-26		107.4
C-27–H_3	1.27	23.9
C-28–H_3	1.41	26.3

Table 6
Measured (Me_2SO-d_6, 25°C) and calculated [25,26] coupling constants $^3J_{H,H}$ of **1**

	Experimental	Calculated	
		X-ray	GROMOS (average)
$J_{31,41}$	2.5	1.0 [a]	1.5 [a] ±0.4
$J_{41,51}$	8.0	8.3 [a]	6.3 [a] ±0.9
$J_{51,61}$	1.0	0.7 [a]	9.5 [a] ±1.1
$J_{51,62}$	1.7	5.0 [a]	5.0 [a] ±0.9
$J_{61,62}$	12.9		
$J_{11,12}$	13.2		
$J_{11,1}$	7.8 [b]	5.3 [b]	4.8±3.6 [b]
$J_{12,1}$	5.5 [b]	0.4 [b]	6.2±3.3 [b]
$J_{71,1}$	9.0	10.6	6.3±3.3
$J_{71,81}$	7 [c]	3.1 [c]	10.4±3.3 [c]
$J_{71,82}$	7 [c]	3.4 [c]	3.7±2.9 [c]

[a] Corrected for electronegativities [25].
[b,c] May be interchanged.

Table 7
NOE connectivities between protons of **1** in Me_2SO-d_6

H-18′/H-22′	H-16′, H-16″
H-101/H-141	H-16′, H-16″, H-81, H-82, H-71
H-11,H-12	H-31
H-31	Me (1.30 ppm), H-1
H-41	Me (1.27 ppm)
H-51	Me (1.27 ppm)
H-62	Me (1.41 ppm)

The coupling pattern of the pyranose ring protons points to the approximately *skew* type conformation of the ring in accordance to those proposed for 2,3:4,5-di-*O*-isopropylidene-β-D-fructopyranose and its acetate [24]. Additionally, a comparison of the experimental $^3J_{H,H}$ couplings of the pyranoid ring with the calculated [25] couplings of the X-ray and the average MD structure (Table 6) shows that the experimental coupling pattern is closer to the X-ray structure. This indicates that in Me_2SO solution the conformation of the pyranoid ring is similar to that of the solid state conformation.

Interesting long range NOE connectivities between the tyrosine protons H-101/H-141 and the benzyl ester protons H-16′, H-16″ were observed, reflecting the conformations with close proximity of the two rings.

Molecular mechanics and dynamics study in vacuo.—The conformational search ended with 571 clusters with (relative) energies ranging from 0.0 to 14.0 kcal/mol. The large number of different clusters with nearly equal energies (starting from 0.0 kcal/mol, there are 13 clusters with energies below 1.0 kcal/mol, 86 below 3.0 kcal/mol and over 278 below 5.0 kcal/mol) imply high flexibility of the molecule.

During simulation the apparent chirality at the pyramidal nitrogen is free to change since no out-of-tetrahedral force field term is used with the aminic group; the value of the torsion angle formed by the atoms N-1–H-1–C-1–C-7 switches from approx. −35° to 35° once each 3–10 ps during dynamics at 500 K.

One of the X-ray structures was found in cluster 239 (sorted by increasing relative energy) with relative energy 4.66 kcal/mol; it violates the NOE constraints. The low-energy structures (rel energy < 3.0 kcal/mol) found with the simulation are in partial or even complete agreement with experimental NOE data.

The sugar part of the molecule is more rigid in the simulation. The average values of cyclic torsion angles are still close to the values found in the crystal, but intermediate

Table 8
The distances (Å) of the four sugar ring protons to the geometrical centres of the isopropylidene methyl groups in the X-ray conformation

H-31–H-25 [a]	3.15
H-41–H-27 [a]	3.19
H-51–H-27 [a]	3.69
H-62–H-28 [a]	4.57

[a] The geometrical centre of the three methyl protons.

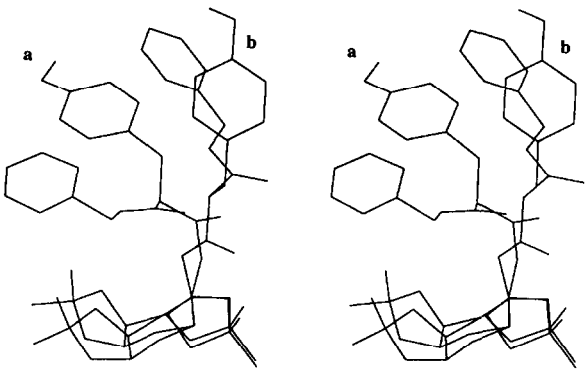

Fig. 3. The stereo diagram of the overlap of the X-ray conformation (a) and the conformation after 1000 ps in molecular dynamics simulations in Me_2SO-d_6 (b).

sofa / half-chair and distorted *chair* conformations of the sugar ring are formed which is a direct consequence of the strong tetrahedral requirements imposed on the ring atoms. The force field used is obviously not suited to correctly reproduce constrained cyclic structures. Since the ring conformation has a negligible effect on the rest of the molecule no correction was applied.

Molecular dynamics simulations with explicit Me_2SO molecules.—In the simulation with explicit solvent molecules the persistence of the X-ray structure in solution was examined. It made a transition to other conformational states and in the course of the observation (1 ns) did not reappear. The superposed X-ray and final MD conformations (after 1000 ps dynamics) are shown in Fig. 3. During the simulation the side chain dihedral angles about the bonds C-1–N-1, N-1–C-7, C-16–C-17 and C-8–C-9 are most flexible and rotamer transitions occur. The C-7–C-8 dihedral angle remains in the *trans* position relative to the main chain throughout the simulation; a large and a small coupling constant for $J_{71,81}$ and $J_{71,82}$ are calculated [26] from the trajectory (Table 6). The estimated experimental values correspond to the expected averaged values of a freely rotating side chain. The agreement of the other calculated and measured side chain spin-spin couplings is also less satisfactory which indicates that even 1 ns dynamics is insufficient for fair simulation of flexible molecules or molecule regions. It must be emphasized that, to the best of our knowledge, no parametrization for the Karplus equation describing amine proton –C-H proton couplings is available; therefore amide proton coefficients were used for $J_{11,1}$, $J_{12,1}$ and $J_{71,1}$ [26].

The distance between the protons H-1 and H-31 that show a long range NOE correlation has been monitored during the simulation and averages to 3.51 Å. The variation of the distances between the protons that show the other long range NOE, H-101/H-141 and H-16′, H-16″, is shown in Fig. 4; both ring protons are never simultaneously close enough to the centre of H-16′, H-16″ to assume a NOE correlation, but one of them most of the time is.

The sugar part is rigid during the simulation (deviations of ring dihedral angles below 8°); the force field again enforces a slightly distorted *chair* conformation of the pyranoid ring.

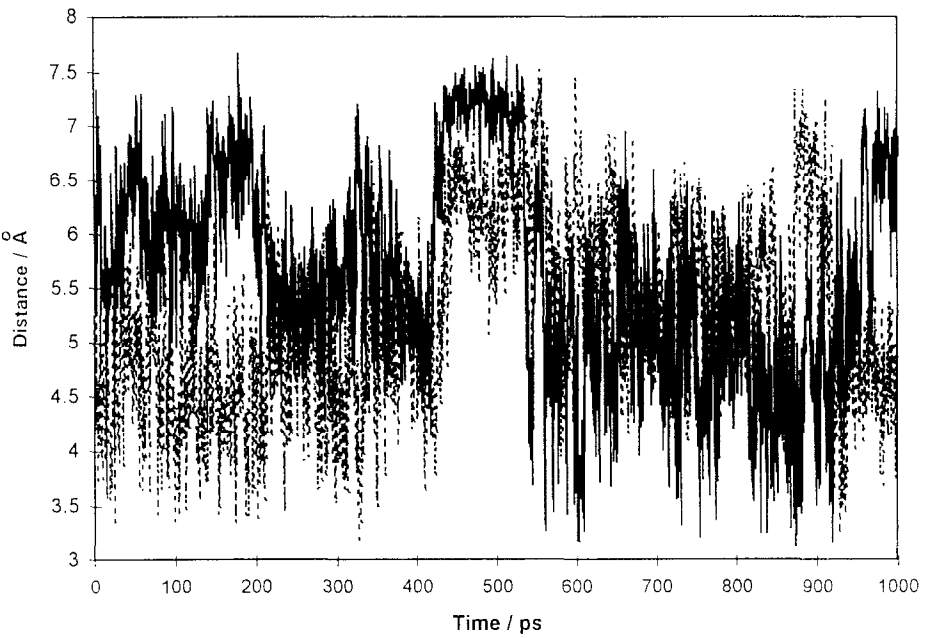

Fig. 4. Trajectory of the distances between H-101–H-16 (dotted line) and H-141–H-16 (solid line) which shows a NOE correlation (H-16 is the geometrical centre of the H-16′/H16″ protons).

The radial distribution functions of the polar hydrogens in the molecule, N-1–H-1 and O-12–H-2, with the solvent oxygens are shown in Fig. 5; O-12–H-2 shows a strong peak of the first solvent layer at ~ 2.7 Å which is indicative of H-bond formation with the oxygen of Me_2SO, and a much weaker second solvent layer at ~ 5.5 Å. Both peaks are much less pronounced with N-1–H-1. The difference in solvent accessibility of both protons is probably one of the reasons for the large differences in the radial distribution functions, the other being the van der Waals's and electrostatic parameters of the atom types involved.

3. Concluding remarks

On the grounds of the large number of energetically nearly equivalent clusters one might conclude that the molecule in Me_2SO-d_6 solution is very flexible and visits many different conformations. The relatively unfavourable energy of the crystal structures in vacuo, their poor agreement with NOE data and their fast transition to other conformations in simulations with explicit solvent suggest that they are not heavily populated in Me_2SO solution; this is not surprising due to the large difference in the surroundings of each molecule which determines the potential for intermolecular interactions in the crystal and in solution.

In the crystal structure the intermolecular hydrogen bonds include the N-1–H-1 group as a donor to the oxygen atom (O-3) of one of dioxolane groups and as an acceptor of

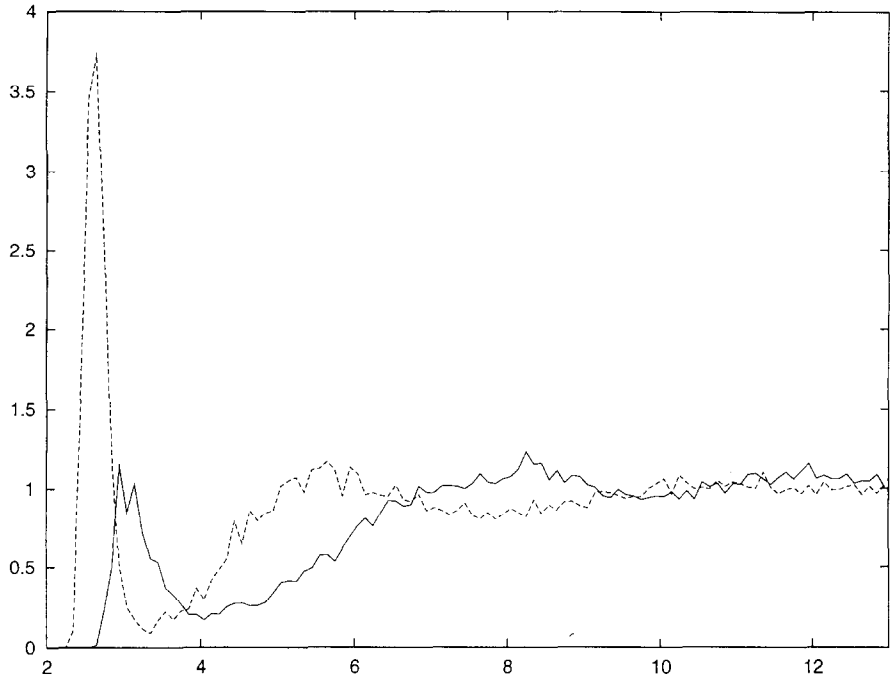

Fig. 5. The radial distribution functions of the polar hydrogens in the molecule, N-1–H-1 (solid line) and O-12–H-2 (dashed line), with the solvent oxygens are shown.

tyrosine hydroxy group (O-12–H-2). However, during the molecular dynamics simulation in Me_2SO intermolecular hydrogen bonds between the tyrosine OH group and the solvent oxygen atoms are more frequent than those between tyrosine amino N–H and solvent oxygen atoms. This finding is in agreement with the hydrogen bonding properties of the amino group.

4. Experimental

General methods.—Melting points were determined on Tottoli (Buchi) melting point apparatus and they were not corrected. Optical rotations were determined with an Optical Activity LTD automatic AA-10 Polarimeter. Column chromatography was performed on silica gel (Merck, 0.063–0.200 mm) and TLC on Silica Gel 60 with detection by ninhydrin, chlorine–iodine reagent or charring with H_2SO_4.

Synthesis of N-*(1-deoxy-2,3:4,5-di-*O*-isopropylidene-β-*D*-fructopyranos-1-yl)*-L-*tyrosine benzyl ester* (**1**).—L-Tyrosine benzyl ester [27] (322 mg, 1.19 mmol), acetic acid (0.088 mL, 1.19 mmol) and sodium cyanoborohydride (78 mg, 1.19 mmol) were added to a solution of 2,3:4,5-di-*O*-isopropylidene-*aldehydo*-β-D-*arabino*-hexos-2-ulo-2,6-pyranose [28] (307 mg, 1.19 mmol) in acetonitrile (2 mL) and tetrahydrofuran (6 mL). The resulting mixture was stirred at room temperature for 4 h. After addition of

Table 9
Crystal data and summary of experimental details

Crystal data	
Molecular formula	$C_{28}H_{35}O_8N$
M_r (g/mol)	513.59
Crystal size (mm)	0.50×0.17×0.22
Crystal system	orthorhombic
Space group	$P\ 2_12_12_1$
a (Å)	10.441(2)
b (Å)	10.894(2)
c (Å)	24.686(4)
V(Å^3)	2808.0(9)
D_x (g/cm^3)	1.22
Z	4
μ(Cu K_α) (cm^{-1})	6.99
F (000)	1096
Data collection	
Difractometer	Enraf-Nonius-CAD4
Radiation	Cu K_α (λ = 1.54184 Å)
Temperature (K)	100
Number of reflection used for cell determination	25
θ_{min}, θ_{max} (°) for cell determination	22, 42
θ_{min}, θ_{max} (°)	3.5, 70
$h\ k\ l$ limits	−12,0; 0,13; 0,30
$\omega/2\theta$ scan (°)	$\Delta\omega = 1.77 + 0.29 \tan\theta$
Reflections measured	3296
Refinement	
Independent reflections observed with $I > 2.5\sigma(I)$	2791
No. of variables	378
R, R_w	0.057, 0.069
Function minimized $\Sigma w(\|F_o\| - \|F_c\|)^2$	$w = \frac{k}{\sigma^2(F_o) - 0.00719F_o^2}$
Max. shift/error $(\Delta/\sigma)_{max}$	−0.086(C25, z)
Residual electron density $(\Delta\rho)_{max}$, $(\Delta\rho)_{min}$ (e/Å^3)	0.27, −0.36

methanol (5 mL), the mixture was concentrated and purified by column chromatography (silica gel; 3:2 benzene–EtOAc) to give **1** (367 mg, 60%) which crystallized from ethanol–water; mp 106–108°C, $[\alpha]_D^{20}$ −26.7° (*c* 1.05, $CHCl_3$). Anal. Calcd for $C_{28}H_{35}NO_8$: C, 65.48; H, 6.87; N, 2.73. Found: C, 65.32; H, 6.84; N, 2.89.

X-ray structure determination of **1**.—Suitable single crystals of **1** were grown by slow crystallization in diisopropyl ether solution. The crystal data and a summary of the experimental details are listed in Table 9. The X-ray intensity data were collected with an Enraf–Nonius CAD4 diffractometer with graphite-monochromatized Cu K_α radiation. During data collection the intensity reduction of standard reflections was about 1.5%. The data were corrected for decay, Lorentz and polarization effects, using the

Enraf–Nonius SDP/VAX package [29]. The structure was solved by SHELX86 [30]. Refinement was by full-matrix least-squares minimizing $\Sigma w(|F_o| - |F_c|)^2$ with the SHELX77 [31] system of programs using F values. The H atom coordinates were determined from successive difference Fourier syntheses; those not being observable were calculated on stereochemical grounds and introduced into the refinement riding on their respective C atoms. In the difference Fourier map two orientations of the benzyloxy group were detected (in Table 10 marked with primes): in the refinement the atoms C-9 to C-14 were treated as rigid groups. The details of the refinement procedure are given in Table 9. In the structure determination, the D enantiomer was selected according to the (*R*) assignment at C-5. Atomic scattering factors were those included in SHELX77 [31]. The molecular geometry was calculated by the program EUCLID [32].

The final atomic coordinates and equivalent isotropic thermal parameters are listed in Table 10 [1]. Calculations were performed on Silicon Graphics INDIGO2 and Micro-VAX-II computers of the X-ray Laboratory, Rudjer Bošković Institute (Zagreb, Croatia).

NMR study.—NMR spectra were obtained on a Varian VXR-300 spectrometer operating at 299.94 MHz for ^{1}H and 75.43 MHz for ^{13}C nuclei. Experiments were performed at 25°C with 50 mM solution in Me_2SO-d_6. At this concentration the association of solute molecules in Me_2SO-d_6 is negligible. Chemical shifts are reported in ppm relative to tetramethylsilane as internal standard. We have used ^{1}H–^{1}H correlation spectroscopy (COSY) [33,34], the DEPT experiment [35], ^{13}C-^{1}H heteronuclear correlation (HETCOR) [36,37] spectroscopy via long range coupling (COLOC) [38] and 2D NOE spectroscopy [39,40] with a standard Varian software. The COSY spectrum was recorded with 512 increments, 32 scans each FID with relaxation delay 2.5 s, the HETCOR spectrum with 512 increments, 64 scans, relaxation delay 2.0 s. The delays in the HETCOR experiment were optimized for $J_{CH} = 140$ Hz. The COLOC spectrum was recorded with 512 increments, 160 scans with relaxation delay 2 s. Delays in the COLOC experiment were optimized for $^nJ_{CH} = 1–10$ Hz. ROESY spectra were recorded with 512 increments, 16 scans, relaxation delays of 2.5 s, and mixing times of 0.25, 0.5, 1.2 and 2.0 s; different transmitter offsets were used in order to identify "false" transverse NOE transfer [41]. Zero filling in t_1 domain and Lorentzian to Gaussian multiplication was used.

Molecular mechanics and dynamics study in vacuo.—The simulations were performed by molecular mechanics based on the consistent valence force-field approach of Lifson and Warshel [42], and Hagler et al. [43,44] incorporated in the molecular simulation package INSIGHT/DISCOVER, version 2.9/3.1 [45]. After initial minimization, 12 starting structures with random values of the torsional angles of the chain residue were allowed 100 ps unrestrained molecular dynamics at 500 K each using the dielectric constant $\epsilon = 46$ (the bulk value of the dielectric constant of Me_2SO); the coordinates were sampled every 0.5 ps and later minimized. The resulting 2400 minimized conformations were clustered according to the values of the torsional angles

[1] The observed and calculated structure factors, H-atom coordinates, and anisotropic thermal parameters have been deposited with the Cambridge Crystallographic Data Centre. The data may be obtained, on request, from the Director, Cambridge Crystallographic Data Centre, 12 Union Road, Cambridge, CB2 1EZ, UK.

Table 10
Final coordinates and equivalent isotropic thermal parameters of the nonhydrogen atoms

Atom	x	y	z	U_{eq} [a] (Å)
O-2	0.3356(2)	0.7790(2)	−0.00140(10)	0.0200(7)
O-3	0.1479(2)	0.7535(2)	−0.04620(10)	0.0190(7)
O-4	0.0725(2)	0.4777(2)	0.02860(10)	0.0183(7)
O-5	0.1916(3)	0.3556(2)	−0.02630(10)	0.0237(8)
O-6	0.3490(2)	0.5697(2)	0.01030(10)	0.0167(7)
O-12	0.5120(3)	0.9353(3)	0.39660(10)	0.0294(9)
O-15	0.4637(3)	0.9402(3)	0.13580(10)	0.0297(9)
O-16	0.2816(3)	0.9081(3)	0.18220(10)	0.0245(8)
N-1	0.4051(3)	0.6766(3)	0.10790(10)	0.0152(8)
C-1	0.2762(4)	0.6843(4)	0.08460(10)	0.020(1)
C-2	0.2778(3)	0.6732(4)	0.02310(10)	0.0171(9)
C-3	0.1397(3)	0.6745(3)	−0.00010(10)	0.0161(9)
C-4	0.0938(3)	0.5494(3)	−0.01900(10)	0.018(1)
C-5	0.1958(3)	0.4745(3)	−0.05010(10)	0.0178(9)
C-6	0.3287(3)	0.5269(4)	−0.04410(10)	0.019(1)
C-7	0.4096(4)	0.7329(3)	0.16220(10)	0.019(1)
C-8	0.5384(4)	0.7066(4)	0.19050(10)	0.022(1)
C-9	0.5399	0.7625	0.2472	0.021(1)
C-10	0.45100	0.72240	0.2855	0.026(1)
C-11	0.4447	0.7791	0.3361	0.028(1)
C-12	0.52730	0.8758	0.3484	0.022(1)
C-13	0.61620	0.9158	0.31010	0.023(1)
C-14	0.6225	0.8592	0.2595	0.025(1)
C-15	0.3911(4)	0.8726(3)	0.15790(10)	0.0171(9)
C-16	0.2581(5)	1.0395(4)	0.1800(2)	0.031(1)
C-17	0.1316(7)	1.0599(9)	0.2004(2)	0.034(4)
C-17′	0.1493(6)	1.0694(6)	0.2221(2)	0.028(3)
C-18	0.0219(7)	1.0626(9)	0.1681(2)	0.049(4)
C-18′	0.0984(6)	1.1876(6)	0.2194(2)	0.029(3)
C-19	−0.0973(7)	1.0855(9)	0.1915(2)	0.060(4)
C-19′	0.0030(6)	1.2235(6)	0.2556(2)	0.052(4)
C-20	−0.1069(7)	1.1058(9)	0.2472(2)	0.076(6)
C-20′	−0.0416(6)	1.1411(6)	0.2946(2)	0.053(4)
C-21	0.0028(7)	1.1031(9)	0.2794(2)	0.14(1)
C-21′	0.0092(6)	1.0229(6)	0.2972(2)	0.065(5)
C-22	0.1220(7)	1.0801(9)	0.2560(2)	0.076(7)
C-22′	0.1047(6)	0.9870(6)	0.2610(2)	0.050(4)
C-23	0.2419(4)	0.8448(4)	−0.0335(2)	0.020(1)
C-24	0.3027(4)	0.8876(4)	−0.0851(2)	0.029(1)
C-25	0.1847(4)	0.9483(4)	0.0007(2)	0.026(1)
C-26	0.0919(4)	0.3524(3)	0.0130(2)	0.021(1)
C-27	−0.0288(4)	0.3000(4)	−0.0113(2)	0.030(1)
C-28	0.1385(5)	0.2842(4)	0.0622(2)	0.034(1)

The tyrosine moiety was treated as a rigid group.
[a] $U_{eq} = (1/3)\Sigma_i \Sigma_j U_{ij} a_i a_j \boldsymbol{a}_i \cdot \boldsymbol{a}_j$.

of the chain residue; deviations of 15° per torsional angle from the running cluster average were tolerated for accepting a conformation as member of the cluster. Computed values of atom–atom distances were compared with measured NOE connectivities.

Molecular dynamics simulations with explicit Me_2SO molecules.—The X-ray structure was used to start an MD simulation with explicit solvent molecules using the program GROMOS [46]. It was soaked with 189 Me_2SO molecules (solute concentration 0.07 M; the Me_2SO box was kindly provided by Dr D. F. Mierke [47]) and minimized with position restraining applied to the solute atoms. Molecular dynamics with periodic boundary conditions using SHAKE (which allowed a step of 2 fs) and tight coupling to a temperature bath (0.01 ps) at 300 K was later initialized and continued for 50 ps; then the coupling was relaxed to 0.1 ps and MD continued for 1000 ps. The coordinates were sampled every 200 steps.

Acknowledgements

This work was supported by Ministry of Science and Technology grants Nos. 1-07-179 and 1-07-192, and The Commission of the European Communities, Brussels, contract No. CI1*-C591-0891. The authors thank Dr Bouke van Eijck, University of Utrecht, Bijvoet Centre for Biomolecular Research for valuable comments and Dr J. C. van Miltenburg, Department of Interfaces and Thermodynamics, University of Utrecht for calorimetric measurements.

References

[1] F. Ledl and E. Schleicher, *Angew. Chem., Int. Ed. Engl.*, 29 (1990) 565–594.
[2] P.A. Finot, H.U. Aeschbacher, R.F. Hurrell, and R. Liardon (Eds.), *The Maillard Reaction* in *Advances in Life Sciences*, Birkhauser, Basel, Switzerland, 1990.
[3] J. Mauron, *Prog. Food Sci.*, 5 (1981) 5–35.
[4] R. Bucala and A. Cerami, *Adv. Pharmacol.*, 23 (1992) 1–34.
[5] K.M. Reiser, M.A. Amigable, and J.A. Last, *J. Biol. Chem.*, 267 (1992) 24207–24216.
[6] M. Brownlee, *Diabetes*, 43 (1994) 836–841.
[7] M.X. Fu, K.J. Wells-Knecht, J.A. Blackledge, T.J. Lyons, S.R. Thorpe, and J.W. Baynes, *Diabetes*, 43 (1994) 676–683.
[8] V.V. Mossine, G.V. Glinsky, and M.S. Feather, *Carbohydr. Res.*, 262 (1994) 257–270.
[9] C.K. Johnson, ORTEP II, Report ORLN-5138, Oak Ridge National Laboratory, Tennessee, USA, 1976.
[10] W.L. Duax, C.M. Weeks, and D.C. Rohrer, *Top. Stereochem.*, 9 (1974) 283–383.
[11] T. Lis and A. Weichsel, *Acta Crystallogr., Sect. C*, 43 (1987) 1954–1956.
[12] IUPAC-IUB Joint Commission on Biochemical Nomenclature (JCBN), *Eur. J. Biochem.*, 111 (1980) 295–298.
[13] J.C.P. Schwartz, *J. Chem. Soc., Chem. Commun.*, (1973) 505–508.
[14] J.C.A. Boeyens, *J. Cryst. Mol. Struct.*, 6 (1978) 317–320.
[15] D. Cremer and J.A. Pople, *J. Am. Chem. Soc.*, 97 (1975) 1354–1367.
[16] J.P.Köll, W. Saax, S. Pohl, B. Steiner, and M. Kooš, *Carbohydr. Res.*, 265 (1994) 237–248.
[17] Cambridge Structural Database System, Version 5.07. Cambridge Crystallographic Data Centre, University Chemical Laboratory, Cambridge, UK, 1994.
[18] F.H. Allen, O. Kennard, D.G. Watson, L. Branmer, A.G. Orpen, and R. Taylor, *J. Chem. Soc., Perkin Trans. 2*, (1987) S1–S19.
[19] W. Klyne and V. Prelog, *Experientia*, 16 (1960) 521–568.
[20] M.G. López and D.W. Gruenwedel, *Carbohydr. Res.*, 212 (1991) 37–45.
[21] H. Röper, S. Röper, K. Heyns, and B. Meyer, *Carbohydr. Res.*, 116 (1983) 183–195.

[22] W. Funcke and A. Klemer, *Carbohydr. Res.*, 50 (1976) 9–13.
[23] M. Bols, *J. Chem. Soc., Chem. Commun.*, (1993) 791–792.
[24] T. Maeda, K. Tori, S. Satoh, and K. Tokuyama, *Bull. Chem. Soc. Jpn.*, 42 (1969) 2635–2647.
[25] M. Budesinsky, T. Trnka, and M. Cerny, *Collect. Czech. Chem. Commun.*, 44 (1979) 1949–1964.
[26] V.F. Bystrov, *Prog. NMR Spectr.*, 10 (1976) 41–81.
[27] R. Wade and F. Bergel, *J. Chem. Soc., (C),* (1967) 592–595.
[28] I.I. Cubero and M.T. Plaza Lopez-Espinosa, *Carbohydr. Res.*, 205 (1990) 293–304.
[29] B.A. Frenz and Associates, Inc. SDP/VAX Structure Determination Package, College Station Texas, USA, 1986.
[30] G.M. Sheldrick, in G.M. Sheldrick, C. Krueger, and R. Goddard (Eds.), *Crystallographic Computing* 3, Oxford University Press, Oxford, UK, 1985.
[31] G.M. Sheldrick, SHELX77, Program for Structure Determination, University of Cambridge, Cambridge, UK, 1983.
[32] A.L. Spek, in D. Sayre (Ed.), *Computational Crystallography*, Clarendon Press, Oxford, UK, 1982, p 528.
[33] G. Bodenhausen, R. Freeman, R. Niedermeyer, and D.L. Turner, *J. Magn. Reson.*, 26 (1977) 133–164.
[34] P. Bachmann, W.P. Aue, L. Mueller, and R.R. Ernst, *J. Magn. Reson.*, 28 (1977) 29–39.
[35] M.R. Bendall, D.M. Dodrell, D.T. Pegg, and W.E. Hull, *DEPT* (1982), Bruker Analytische Messtechnik, Karlsruhe.
[36] A. Bax and G.A. Morris, *J. Magn. Reson.*, 42 (1981) 501–505.
[37] A. Bax, *J. Magn. Reson.*, 53 (1983) 517–520.
[38] H. Kessler, C. Greisinger, J. Zarbock, and H.R. Loosli, *J. Magn. Reson.*, 57 (1984) 331–336.
[39] S. Macura, Y. Huang, D. Suter, and R.R. Ernst, *J. Magn. Reson.*, 43 (1981) 259–281.
[40] J.D. States, R.A. Haberkorn, and D.J. Ruben, *J. Magn. Reson.*, 48 (1982) 286–292.
[41] D. Neuhaus and J. Keeler, *J. Magn. Reson.*, 68 (1986) 568–574.
[42] S. Lifson and A. Warshel, *J. Chem. Phys.*, 49 (1969) 5116–5129.
[43] A.T. Hagler, Z. Huler, and S. Lifson, *J. Am. Chem. Soc.*, 96 (1974) 5319–5327.
[44] A.T. Hagler, L. Lifson, and P. Dauber, *J. Am. Chem. Soc.*, 101 (1979) 5122–5130.
[45] BIOSYM. INSIGHT/DISCOVER, version 2.9/3.1, Biosym Technologies (10065 Barnes Canyon Rd., San Diego, CA 92121, USA, 1993.
[46] W.F. van Gunsteren, GROMOS, Groningen, Molecular Simulation Computer Program Package, University of Groningen, The Netherlands, 1987.
[47] D.F. Mierke and H. Kessler, *J. Am. Chem. Soc.*, 113 (1991) 9466–9470.